Acadlore Transactions on Applied Mathematics and Statistics
https://www.acadlore.com/journals/ATAMS

Vibrational Response of a Continuous System: Analysis of Elastic Bar Behavior under Multiple Boundary Conditions

Umara Bushra[1], Talha Anwar[2*], Asifa[3]

[1] Department of Mathematics, COMSATS University Islamabad, 45550 Islamabad, Pakistan
[2] School of Science, Walailak University, 80160 Nakhon Si Thammarat, Thailand
[3] Center of Excellence in Theoretical and Computational Science (TaCS-CoE), Science Laboratory Building, Faculty of Science, King Mongkut's University of Technology Thonburi (KMUTT), 10140 Bangkok, Thailand

* Correspondence: Talha Anwar (anwartalha80@gmail.com)

Received: 01-31-2025 **Revised:** 03-15-2025 **Accepted:** 03-27-2025

Citation: U. Bushra, T. Anwar, and Asifa, "Vibrational response of a continuous system: Analysis of elastic bar behavior under multiple boundary conditions," *Acadlore Trans. Appl Math. Stat.*, vol. 3, no. 1, pp. 65–82, 2025. https://doi.org/10.56578/atams030105.

Abstract: This study presents a vibrational analysis of an elastic bar, a fundamental element in continuous systems. The primary objective is to evaluate the vibrational response of a uniform elastic bar under various boundary conditions, including Dirichlet, Neumann, and mixed types. Both numerical and analytical techniques—specifically the finite element method (FEM) and the method of separation of variables—are employed to determine the eigenfrequencies and mode shapes of the bar. The governing equation for a uniform torsional bar, along with its natural boundary conditions, is formulated and solved using separation of variables, leading to coupled equations. Solutions are derived for multiple end conditions, and dispersion (frequency) equations are obtained to compute the eigenvalues. Root-finding methods are used to extract natural frequencies and corresponding eigenfunctions. The vibrational response is visualized for different cases and compared with existing results in the literature. Findings reveal that the natural frequencies of torsional bars are affected by additional elements such as attached masses, springs, and dampers. This investigation enhances the understanding of elastic bar dynamics and provides useful insights for the design and optimization of structural systems involving torsional bars.

Keywords: Elastic bar; Natural frequencies; Frequency equation; Eigen functions; Dispersive relations; Finite element method (FEM)

1 Introduction

The vibration issues pertinent to the high-speed formations and the development at large scales, for instance, mechanical and structural systems, aerospace, medical machines, underwater vehicles, etc., must be critically examined and treated for the proper working of such structures and machinery. Moreover, intricate surrounding loads and environmental impacts may also lead to arising vibration challenges. Consequently, various fields require an all-inclusive investigation of vibrating bars, such as industrial automation and manufacturing, transport engineering, measurement and sensor devices, ultrasonics, mechanical engineering, structural development, and so forth. In addition, researchers are also focused on vibration amplitude controlling techniques and methods to efficaciously cope with any odd challenges.

The profound contributions of Newton's second law of motion, Hooke's fundamental law of elasticity, and Leibniz's concepts of differential calculus are all intricately linked to the study of vibration in continuous systems. In modern vibration literature, the equations of motion for vibrating bodies are typically derived using Newton's second law of motion. Vibration is one of the most interesting phenomena in the universe that plays an important role in many real-world problems [1, 2]. It is defined as a repetitive motion around an equilibrium point. It is imperative to understand vibratory motion for safe designs, construction, and various other operations of machines [3]. Vibration has numerous applications in every field of life, such as sound navigation, acoustics, biomedical, automotive, and musical fields. Dynamical imbalance of structures may cause excessive vibration which further yields multiple types of failures in components [4]. It is worthwhile to have a theoretical study of how bars, strings, beams, plates, membranes, and other continuous structures vibrate. Also, the vibration of a continuous system is an ideal subject for discussing partial differential equations and eigenvalue problems [5]. This article discusses the vibration phenomena of elastic bars. Bars are the fundamental component of continuous systems that can deform both longitudinally (where the bar acts like a rod) and torsionally. It is essential to use continuous elastic bars while investigating structural vibrations. The study of elastic bars helps in evaluating the stability of structures under different loading conditions. This is particularly important in ensuring that buildings and bridges remain safe under various stress conditions such as earthquakes and heavy traffic loads [6, 7].

Torsional dynamics of the bar are significantly considered in the case of curved bridges. It is essential to examine it as the angular bar vibrations highly impact the safety, functioning, and overall potential of the systems. In the case, where structures are composed of rotating components, the torsional dynamics become crucial [8]. To avoid over bending in pipelines and risers that are mostly used in industry, models of elastic flexible bars based on stress-strain relationships, are used [9]. Torsional vibrations in elastic bars have many applications in vehicles like modern cars and other military vehicles. Due to the rotational effect, it enables them to absorb road shocks and helps to detect cracks in machinery. Some critical analyses of torsional vibrations in transportation engineering can be observed in the studies [10, 11]. Apart from this, torsional vibrations also play a vital role in high-speed machinery and help them to transmit power [12]. Various reports have been included in the data about the torsional vibration and its significance with respect to practical functioning. Chen et al. [13] explicated different techniques to suppress the torsional vibrations because it might seriously damage or affect the safety, reliability, and efficient working of hybrid vehicles. They proposed several controllers for limiting the torsional vibrations. An analytic model for explicating the torsional fluctuations was computed by Chen and Hu [14]. They made analytic calculations and suggested a method to control the torsional fluctuations. Resultantly, they achieved a method, that is of extreme significance for suppressing rotational fluctuations in electric vehicles. Tariq et al. [15] introduced machine learning and semi-exact strategies for studying the viscoelastic nanotubes. They derived frequencies utilizing elestic conditions and evaluated behaviors under torsional vibrations. Sharma et al. [16] made the drilling vibrations their topic of discussion and chewed over several techniques that could be helpful in diminishing such vibrations. Otherwise, they could result in elevated drilling costs and machine dysfunctions, and there may arise productivity issues and safety concerns. Sharma et al. [16] reviewed all types of possible vibrations during drilling and proposed some vital controlling tools and mitigating techniques.Ledezma-Ramírez et al. [17] reviewed multiple recent advancements and future possibilities of shock vibrations. Some new observations about torsional vibration can be studied from the studies [18–25].

The longitudinal properties of the bar are also of extreme significance regarding several applications, for instance, designing engineering systems, uses of ultrasonic waves for the detection of internal flaws, mechanical systems, acoustics, material science, and many others. The precise anticipation of these vibrations improves the understanding of consequences eventuated by behavioral shifts, which assists in forecasting the influences of various loading conditions on the response of structures and materials. The foundational work in the field of vibrations is on the credit of Newton and Galileo. However, the noteworthy development in this regard took place because of the general elasticity theory, propounded by Claude-Louis Navier. It opened the possibility of inspecting elastic bodies in order to analyze vibrations. The mathematical setting formulated by Navier enabled the description of elastic solids' movement, which holds a significant contribution in comprehending longitudinal vibrations. To date, researchers have focused on multiple aspects of longitudinal vibrations and made important reports. Coulomb studied the torsion balance while investigating the torsion of circular cylinders, and after integrating it, he found that the oscillation period is independent of the angle of twist. The groundbreaking work of Poisson's on wave propagation and elasticity is considered one of the foundational works. It provided a necessary ground for further advancements of the research domain. Love [26] utilized Poisson idea of longitudinal vibration of the rod by including inertial effects and also incorporating warping effects in torsional dynamics. The studies [27, 28] have made detailed studies about the vibrations of bars. An exclusive analysis of free vibrations was carried out by Ke et al. [29]. They conducted exhaustive work explaining several key parameters, for example, aspect ratio, size effect parameter, and length-to-thickness ratio. Akgöz and Civalek [30] employed Hamilton's theory to derive an equation of motion for scrutinizing several mechanisms influencing the vibrational response of a micro-scale bar. Dimosthenis [31] assessed multiple factors, including BCs, attachments, the bar's length and the parameter indicating internal length, and modes, for observing vibrational changes. A few more discussions on this subject are recorded in the researches [32–39].

According to the references discussed so far, numerous authors have worked on approaches similar to this one, but some gaps remain, such as their failure to address the effects of mass, springs, and dampers on the ends of the bar. The underlying study describes how to analyze the behavior of an elastic bar subject to classical boundary conditions using the separation of variables method and the finite element method (FEM). A modal analysis of the bar with attached masses, springs, and dampers at one or both ends is included in the study. Moreover, non-classical boundary conditions—as opposed to the well-researched classical boundary conditions—are considered in the suggested models. It is important to note that the underlying research is novel in that it looks for more accurate and efficient ways to solve the underlying problem, as well as using non-classical boundary conditions. Without taking into account any external forces, it is demonstrated that the FEM converges efficiently to the exact solution. The study also shows that natural frequencies rise in the presence of masses, springs, dampers, and foundation constants. While previous studies have focused on numerical solutions for the impacts of dampers, masses, and springs on a bar's mode shapes, this work stands out for taking into account the effects of multiple foundations as well as torsional bars, each of which has non-classical limitations. It differs from earlier efforts in that it takes a complete approach. Establishing a productive interaction between several components is the main goal. Notably, the natural frequency of the bars is significantly influenced by the type of foundation that is chosen—mass, springs, or dampers—with the relative stiffness of the foundation and the bar acting as a key factor in this decision. The unique focus of this study on these features advances our knowledge of structural behavior under various settings and makes a significant contribution to the discipline. Consequently, the research provides a significant understanding of bar behavior under different foundation conditions, paving the way for further studies on higher bar theories and improved models, and investigating the impact of different boundary conditions and foundations. These results advance our knowledge of bar analysis and its uses in structural optimization and design. The novelty of this analysis is highlighted by listing below the key points of this investigation:

- The acquisition of exact expressions is aimed at exercising the separation of variables method.
- The comparison evaluations are conducted by solving the system by dint of the FEM.
- The response of the bar based on several types of attached materials is noted.
- The behavioral shifts are reported for one end attachment as well as both end attachments.
- The solutions subject to non-classical constraints are equated with those secured via classical conditions.
- Natural frequencies are elucidated by computing the eigenfunctions.

This is how the rest of the article is structured. Section 2 presents the governing problem. A working method for determining eigenvalues, eigenmodes, and eigenfrequencies is provided in Section 3. Section 4 presents and discusses the findings, while Section 5 offers the conclusion.

2 Statement of Problem

Consider the torsional vibrations of a bar with length l consisting of each cross section along the longitudinal axis passing through the centroid of the cross section as shown in Figure 1.

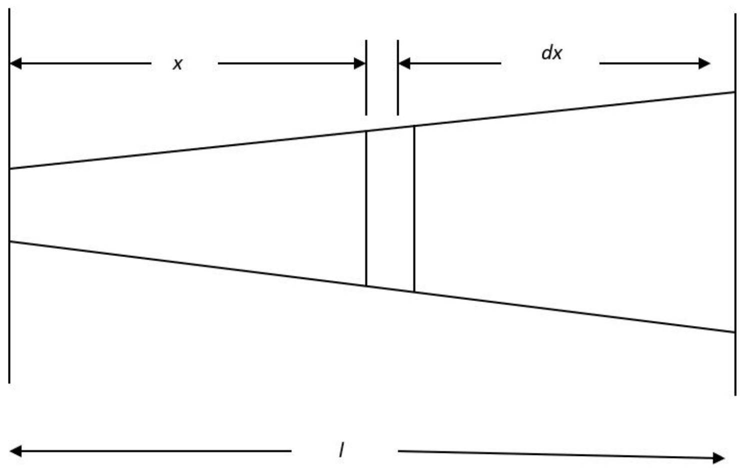

Figure 1. Configuration of elastic bar

The equation of motion for a uniform torsional bar in the absence of external torsional moments is given by

$$k_\phi G_x \frac{\partial^2 \phi}{\partial x^2} = \rho P_I \frac{\partial^2 \phi}{\partial t^2} \tag{1}$$

where, $\phi(x,t)$ represents the displacement of transverse vibrations of bar from the equilibrium position, and k_ϕ, G_x, ρ, P_I are torsion stiffness coefficient, shear modulus for the material, mass per unit volume, and polar area moment of inertia of cross section, respectively. In this article, we will discuss the vibrations of the torsional bar under different sets of boundary conditions given as follows:

Fixed ends:

$$\phi(0,t) = \phi(L,t) = 0 \tag{2}$$

Fixed-free ends:

$$\phi(0,t) = \phi'(L,t) = 0 \tag{3}$$

Free ends:

$$\phi'(0,t) = \phi'(L,t) = 0 \tag{4}$$

Vibrations of bar with left end fixed and attached mass at right end:

$$\begin{aligned} \phi(0,t) &= 0 \\ k_\phi G_x \frac{\partial \phi(L,t)}{\partial x} &= -M \frac{\partial^2 \phi(L,t)}{\partial t^2} \end{aligned} \tag{5}$$

Vibrations of bar with right end fixed and attached mass at left end:

$$\begin{aligned} k_\phi G_x \frac{\partial \phi(0,t)}{\partial x} &= M \frac{\partial^2 \phi(0,t)}{\partial t^2} \\ \phi(L,t) &= 0 \end{aligned} \tag{6}$$

Vibrations of bar with left end free and attached mass at right end:

$$\begin{aligned} \frac{\partial \phi(0,t)}{\partial x} &= 0 \\ k_\phi G_x \frac{\partial \phi(L,t)}{\partial x} &= -M \frac{\partial^2 \phi(L,t)}{\partial t^2} \end{aligned} \tag{7}$$

Vibrations of bar with right end free and attached mass at left end:

$$\begin{aligned} k_\phi G_x \frac{\partial \phi(0,t)}{\partial x} &= M \frac{\partial^2 \phi(0,t)}{\partial t^2} \\ \frac{\partial \phi(L,t)}{\partial x} &= 0 \end{aligned} \tag{8}$$

Vibrations of bar with attached mass at both ends:

$$\begin{aligned} k_\phi G_x \frac{\partial \phi(0,t)}{\partial x} &= M_1 \frac{\partial^2 \phi(0,t)}{\partial t^2} \\ k_\phi G_x \frac{\partial \phi(L,t)}{\partial x} &= -M_2 \frac{\partial^2 \phi(L,t)}{\partial t^2} \end{aligned} \tag{9}$$

Vibrations of bar with left end fixed and attached mass and springs at right end:

$$\begin{aligned} \phi(0,t) &= 0 \\ k_\phi G_x \frac{\partial \phi(L,t)}{\partial x} &= -M \frac{\partial^2 \phi(L,t)}{\partial t^2} - k_t \phi(L,t) \end{aligned} \tag{10}$$

Vibrations of bar with left end free and attached mass and springs at right end:

$$\begin{aligned} \frac{\partial \phi(0,t)}{\partial x} &= 0 \\ k_\phi G_x \frac{\partial \phi(L,t)}{\partial x} &= -M \frac{\partial^2 \phi(L,t)}{\partial t^2} - k_t \phi(L,t) \end{aligned} \tag{11}$$

Vibrations of bar with attached mass and springs at both ends:

$$\begin{aligned} k_\phi G_x \frac{\partial \phi(0,t)}{\partial x} &= M_1 \frac{\partial^2 \phi(0,t)}{\partial t^2} + k_{1t} \phi(0,t) \\ k_\phi G_x \frac{\partial \phi(L,t)}{\partial x} &= -M_2 \frac{\partial^2 \phi(L,t)}{\partial t^2} - k_{2t} \phi(L,t) \end{aligned} \tag{12}$$

Vibrations of bar with attached mass, springs, and dampers at both ends:

$$\begin{aligned} k_\phi G_x \frac{\partial \phi(0,t)}{\partial x} &= M_1 \frac{\partial^2 \phi(0,t)}{\partial t^2} + d_1 \frac{\partial \phi(0,t)}{\partial t} + k_{1t} \phi(0,t) \\ k_\phi G_x \frac{\partial \phi(L,t)}{\partial x} &= -M_2 \frac{\partial^2 \phi(L,t)}{\partial t^2} - d_2 \frac{\partial \phi(L,t)}{\partial t} - k_{2t} \phi(L,t) \end{aligned} \tag{13}$$

Here, L is the length of an elastic bar. Also, it is important to mention here that Eqs. (2)-(4) represent classical boundary conditions of a bar subject to fixed, fixed-free, and free ends. Eqs. (5)-(8) represent boundary conditions of the torsional bar, whose one end is fixed or free, and mass M is attached at the other end, and Eq. (9) represents vibrations of the bar with attached masses on both ends. Similarly, Eq. (10) and Eq. (11) represent the vibration of a torsional bar with one end fixed or free with both mass and spring are attached at the other end, and Eq. (12) represents the vibration of a torsional bar with both mass and spring attached at both ends. Now, Eq. (13) represents boundary conditions of the bar having certain masses M_1 and M_2, supported by linear springs having stiffness coefficients k_{1t} and k_{2t} along with linear damping d_1 and d_2, respectively. The method for calculating eigenfrequencies and eigen modes is explained analytically and numerically in the next section.

3 Determination of Eigen Modes and Natural Frequencies

Torsional vibrations have a wide range of importance in industrial-scale because many machines used in industry are rotational in nature. These vibrations are more complex as they are harder to detect. So, it is most important to determine the natural frequencies of a system because the amplitude of vibration rises significantly when the speed of the system gets closer to its natural frequency.

The foremost important task in any vibrating system is to determine its natural frequencies and mode shapes. Natural frequencies allow the system to vibrate when it is subject to certain disturbances. The deformed shape of any structure at specific natural frequencies is known as the mode shape. The determination of natural frequencies and mode shapes depends on the choice of boundary conditions and structural properties. In this section, we are going to analyse mode shapes and natural frequencies of uniform bar subjects under different end conditions.

3.1 Analytic Solution

If a body is given torque, and when this torque is released, it performs vibration, which is known as torsional vibration. Free vibrations occur due to some initial disturbance that causes the system to oscillate under the action of forces acting on a system, and when the externally applied forces are absent. Here, we will discuss the problem in the absence of external moments or free vibrations of the bar. The technique that we intend to use in order to solve the problem is the separation of a variable [40].

With the help of the method of separation of variables, Eq. (1) can be solved by letting:

$$\phi(x,t) = S(x)R(t) \tag{14}$$

The following expressions can be conveniently acquired from Eq. (14):

$$\frac{\partial^2\phi(x,t)}{\partial x^2} = R(t)S''(x) \text{ and } \frac{\partial^2\phi(x,t)}{\partial t^2} = R''(t)$$

Putting the above expressions in Eq. (1) yields:

$$(k_\phi G_x)\, S''(x)R(t) = (\rho P_I)\, S(x)R''(t) \tag{15}$$

On combining the terms with the same independent variables, Eq. (15) takes the following shape:

$$\frac{S''(x)}{S(x)} = E^2\frac{R''(t)}{R(t)} = -\beta^2 \tag{16}$$

Here, $E^2 = \frac{\rho P_I}{k_\phi G_x}$ and β is some arbitrary constant. ρ and P_I are mass per unit volume and polar area moment of inertia of the cross section, and their product defines mass distribution, which occurs in dynamical torsional systems. k_ϕ describes the material stiffness, and G_ϕ indicates the torsional resistance. Their product characterizes the torsional restoring force, which will be dominant for a high product value.

Eq. (16) can be converted into the form of two ODEs as:

$$S''(x) + \beta^2 S(x) = 0 \tag{17}$$

$$R''(t) + \gamma^2 R(t) = 0 \tag{18}$$

where,

$$\gamma^2 = \frac{k_\phi G_x \beta^2}{\rho P_I} \tag{19}$$

The corresponding solutions of the spatial variable and time-dependent Eq. (17) and Eq. (18) are given as:

$$S(x) = A\cos(\beta x) + B\sin(\beta x) \tag{20}$$

$$R(t) = C\cos(\gamma t) + D\sin(\gamma t) \tag{21}$$

Here, the coefficients A and B are obtained through boundary conditions. Eq. (20) is known as the fundamental equation for the torsional bar, as it contains the information of natural frequencies and mode shapes. The coefficients C and D are obtained through initial conditions. It involves harmonic motion at the corresponding natural frequency, which is

$$\gamma_m = \sqrt{\frac{k_\phi G_x}{\rho P_I}}\beta_m, m = 0, 1, 2, 3, ... \tag{22}$$

where, γ_m is known as the eigenfrequency or natural frequency of a bar. The complete vibrational response is given by:

$$\phi_n(x,t) = \sum_{n=0}^{\infty}\left[C_n\cos(\gamma t) + D_n\sin(\gamma t)\right]S_n(x) \tag{23}$$

The unknown coefficients C_n and D_n are obtained through initial conditions, and coefficients of spatial variables are determined through boundary conditions. Now, we will use the different boundary conditions mentioned before to find solutions.

Eigenvalues and eigenfunctions of fixed-fixed bars:

Using Eq. (2) in Eq. (20) with the help of Eq. (14) yields the corresponding frequency equation or characteristic equation of a system and eigenvalues of a fixed-fixed bar [41]:

$$B\sin\beta(L) = 0, \beta_m = \frac{m\pi}{L}, m = 0, 1, 2, 3, \ldots \tag{24}$$

Using Eq. (24) in Eq. (22) yields eigenfrequencies of the form:

$$\gamma_m = \frac{m\pi}{L}\sqrt{\frac{k_\phi G_x}{\rho P_I}} \tag{25}$$

and the corresponding eigenfunction is of the form:

$$S_m(x) = B_m\sin\beta_m x \tag{26}$$

Eigenvalues and eigenfunctions of fixed-free bar:

Now, using the boundary condition given in Eq. (3) yields the characteristic equation or frequency equation with an eigenfrequency of the form:

$$\cos\beta(L) = 0 \tag{27}$$

$$\beta_m = \left(m - \frac{1}{2}\right)\frac{\pi}{L}, m = 1, 2, 3, ... \tag{28}$$

and eigenfunction for the fixed-free bar is:

$$S_m(x) = B_m\sin\beta_m x, m = 1, 2, 3, ... \tag{29}$$

Eigenvalues and eigenfunctions of free bar:

Now, the corresponding characteristic equation and eigenfunctions for the free ends of the torsional bar is given as:

$$\sin\beta(L) = 0 \tag{30}$$

$$S_m(x) = A_m \cos\beta_m x, m = 0, 1, 2, 3, ... \tag{31}$$

The corresponding eigenfunctions and frequency equations for the fixed torsional bar having attached masses at either end are given as:

Attached mass at right end:

Eigenfunctions and frequency equations for boundary conditions given in Eq. (5) are referred to as:

$$S(x) = B\sin(\beta x) \tag{32}$$

$$\tan\alpha - \frac{\lambda}{\alpha} = 0 \tag{33}$$

where,

$$\alpha = \beta L, \lambda = \frac{\rho P_I L}{M}$$

Attached mass at left end:

Eigenfunctions and frequency equations for boundary conditions given in Eq. (6) are referred to as:

$$S_n(x) = B[-\tau_n\cos(\beta_n x) + \sin(\beta_n x)] \tag{34}$$

and the frequency equation is the same as given in Eq. (33), where, the characteristic parameter τ_n is defined as:

$$\tau_n = \tan\alpha_n$$

Eigen functions and frequency equations for the free torsional bar having attached masses at either end are given as:

Attached mass at right end:

Eigen functions and frequency equations for boundary conditions given in Eq. (7) are referred to as:

$$S(x) = A\cos(\beta x) \tag{35}$$

$$\tan\alpha + \frac{\alpha}{\lambda} = 0 \tag{36}$$

Attached mass at left end:

Eigenfunctions and frequency equations for boundary conditions given in Eq. (8) are referred to as:

$$S_n(x) = A[\cos(\beta x) + \tau_n\alpha\sin(\beta x)] \tag{37}$$

and frequency equation is as given in Eq. (36).

Torsional bar with attached mass at both ends:

Eigen functions and frequency equations for boundary conditions given in Eq. (9) are referred to as:

$$S_n(x) = A_n[\cos(\beta_n x) - \tau_n\sin(\beta_n x)] \tag{38}$$

and the dispersive relation of a torsional bar having masses is attached at both ends, is of the form:

$$\tan\alpha = \left[\frac{\alpha\lambda_1 + \alpha\lambda_2}{\alpha^2 - \lambda_1\lambda_2}\right] \tag{39}$$

where,

$$\lambda_1 = \frac{\rho P_1 L}{M_1}, \lambda_2 = \frac{\rho P_1 L}{M_2}$$

Since there exists an eigenfunction corresponding to each eigenvalue. So, eigenvalues are obtained through the root-finding process.

Now, Eq. (10) and Eq. (11) represent boundary conditions for a torsional bar having one end fixed or free, and a certain mass M and stiffness of spring k_t are attached at its other end at $x = L$, respectively. The zero displacement at the first end and a certain mass M and spring are attached to the other end of a bar because of which, the rigidity occurs, and the slope of a bar, inertial forces, and displacement are said to be equal. So, corresponding eigenfunctions and dispersive relations are given as:

Vibrations of fixed torsional bar at left end:

$$
\begin{aligned}
S(x) &= B\sin(\beta x)\\
\alpha\cot\alpha &= \frac{\alpha^2}{\lambda} - \frac{k_t}{k_0}
\end{aligned} \tag{40}
$$

Vibrations of free torsional bar at left end:

$$
\begin{aligned}
S(x) &= A\cos(\beta x)\\
\alpha\tan\alpha &= \frac{k_t}{k_0} - \frac{\alpha^2}{\lambda}
\end{aligned} \tag{41}
$$

Since eigenvalues are not determined explicitly, we use root-finding techniques to evaluate them.

Now Eq. (12) represents boundary conditions of the torsional bar with certain masses and linear springs attached at both of its ends. We consider transverse displacement $\phi(x,t)$ and acceleration $\frac{\partial^2\phi(x,t)}{\partial t^2}$ to be positive. The inertial force $M_1\phi_{tt}(0,t)$ and spring force $k_{1t}(0,t)$ act upward. At $x=0$, the positive slope of the bar is equal to positive spring forces and inertia. While at $x=L$, the inertial force $M_2\phi_{tt}(L,t)$ and spring force $k_{2t}(L,t)$ acts downward. Also, at $x=L$, the positive slope of the bar is equal to the negative of the forces of spring and inertia. Now, the corresponding characteristic eigenfunction and dispersive relation of a bar in this case is given as:

$$
S_n(x) = B_n\Big(\tau_n\cos(\beta_n x) + \sin(\beta_n x)\Big) \tag{42}
$$

$$
\begin{aligned}
&\frac{\alpha^3}{\lambda_1} - \frac{\alpha^2}{\lambda_1}\tan\alpha\left(\frac{\alpha^2}{\lambda_2} - \frac{k_{2t}}{k_0}\right) - \alpha\frac{k_{2t}}{k_0}\\
&+\frac{k_{1t}}{k_0}\tan\alpha\left(\frac{\alpha^2}{\lambda_2} - \frac{k_{2t}}{k_0}\right) + \alpha^2\tan\alpha + \alpha\left(\frac{\alpha^2}{\lambda_2} - \frac{k_{2t}}{k_0}\right) = 0
\end{aligned} \tag{43}
$$

and the characteristic parameter is given as:

$$
\tau_n = \frac{\left[\alpha_n\cos\alpha_n - \sin\alpha_n\left(\frac{\alpha_n^2}{\lambda_2} - \frac{k_{2t}}{k_0}\right)\right]}{\left[\cos\alpha_n\left(\frac{\alpha_n^2}{\lambda_2} - \frac{k_{2t}}{k_0}\right) + \alpha_n\sin\alpha_n\right]}
$$

Now, we aim to determine torsional vibrations of a bar having certain masses M_1 and M_2, supported by linear springs having stiffness coefficients k_{1t} and k_{2t} along with linear damping d_1 and d_2, respectively and corresponding boundary conditions are given in Eq. (13). Since viscous damping is involved in our model, assume the solution is of the form:

$$
\phi(x,t) = S(x)e^{\xi t} \tag{44}
$$

Here, ξ is an eigenvalue, which is complex in general. Now, using Eq. (44) in Eq. (1), and after certain simplifications, we get:

$$
S(x) = A\cos(\omega x) + B\sin(\omega x) \tag{45}
$$

Here, ξ_n is the complex eigenvalue, so corresponding to this complex eigenvalue, we have complex eigen frequency ω_n of the form:

$$
\omega_n = \iota\sqrt{\frac{k_\phi G_x}{\rho P_I}}\xi_n \tag{46}
$$

Also, the corresponding frequency equation of the torsional bar having masses, springs, and dampers attached at each end, is of the form:

$$
\begin{aligned}
&\frac{\psi^2}{\lambda_1\lambda_2}\tan\psi + \frac{d_2\psi}{\mu\lambda_1}\iota\tan\psi + \frac{k_{2t}}{k_0\lambda_1}\tan\psi - \frac{\psi}{\lambda_1}\\
&-\frac{d_1\psi}{\mu\lambda_2}\iota\tan\psi + \frac{d_1 d_2}{\mu^2}\tan\psi - \frac{k_{2t}d_1}{k_0\psi\mu}\iota\tan\psi - \frac{d_1}{\mu}\iota\\
&-\frac{k_{1t}}{k_0\lambda_2}\tan\psi - \frac{k_{1t}d_2}{k_0\psi\mu}\iota\tan\psi - \frac{k_{1t}^2}{k_0^2\psi^2}\tan\psi - \frac{k_{1t}}{k_0\psi}\\
&+\tan\psi - \frac{\psi}{\lambda_2} - \frac{d_2}{\mu}\iota + \frac{k_{2t}}{k_0\psi} = 0
\end{aligned} \tag{47}
$$

Also, we have an eigenfunction of the form:

$$S(x) = B\left[\frac{\frac{\psi}{\lambda_2}\sin\psi + \frac{d_{2t}}{\mu}\sin\psi + \frac{k_{2t}}{k_0\psi}\sin\psi + \cos\psi}{\sin\psi - \frac{\psi}{\lambda_2}\cos\psi - \frac{d_{2t}}{\mu}\cos\psi - \frac{k_{2t}}{k_0\psi}\cos\psi}\cos(\beta x) + \sin(\beta x)\right] \tag{48}$$

The complex characteristic parameter is defined as:

$$\eta_n = \frac{\frac{\psi}{\lambda_2}\sin\psi + \frac{d_{2t}}{\mu}\sin\psi + \frac{k_{2t}}{k_0\psi}\sin\psi + \cos\psi}{\sin\psi - \frac{\psi}{\lambda_2}\cos\psi - \frac{d_{2t}}{\mu}\cos\psi - \frac{k_{2t}}{k_0\psi}\cos\psi}$$

Now, in the next section, we will analyse numerical solutions of transcendental equations, also the graphical and tabular representation of mode shapes will be discussed.

4 Results and Discussion

The main goal of this section is to illustrate the modal analysis of torsional bars that are elastically limited by connected mass, linear springs, and viscous dampers. The cross-sectional dimensions of the bars under examination are consistent. This section's main goal is to demonstrate how these torsional bars behave modally and how they react to outside forces under different foundation conditions. Eq. (1), which represents torsional dynamics, was utilized for this purpose. For distinct model analyses, a variety of parameters were employed, and each behavior is listed below.

4.1 Graphical and Tabular Representation

Here, Table 1 and Table 2 given below present corresponding eigenvalues and natural frequencies of a bar subject to fixed and fixed-free ends with $L = 1$, $K_\phi = 0.1$, $G_x = 0.2$, $\rho = 1$, and $P_I = 0.9$, respectively.

Table 1. Eigenvalues and natural frequencies of fixed bar

m	$\beta_m = \frac{m\pi}{L}$	γ_m
1	π	0.46808
2	2π	0.936
3	3π	1.4043
4	4π	1.87239
5	5π	2.3404
6	6π	2.808
7	7π	3.2766
8	8π	3.7447
9	9π	4.2128
10	10π	4.6809

Table 2. Eigenvalues and natural frequencies of fixed-free bar

m	$\beta_m = \frac{(2m-1)\pi}{2L}$	γ_m
1	$\frac{\pi}{2}$	0.2342
2	$\frac{3\pi}{2}$	0.7025
3	$\frac{5\pi}{2}$	1.1708
4	$\frac{7\pi}{2}$	1.6391
5	$\frac{9\pi}{2}$	2.1074
6	$\frac{11\pi}{2}$	2.5757
7	$\frac{13\pi}{2}$	3.044
8	$\frac{15\pi}{2}$	3.5124
9	$\frac{17\pi}{2}$	3.9807
10	$\frac{19\pi}{2}$	4.4490

Now, Table 1 and Table 2 represent the first few eigenvalues and natural frequencies of fixed-fixed and fixed-free bars, also Table 3 shows that the eigenvalues and natural frequencies of free-free bars are similar to those of fixed-fixed bars. Now, the below graphs represent the mode shapes of the fixed, fixed-free, and free ends of a bar.

We obtained an explicitly defined eigenvalue, and corresponding to each eigenvalue, we get an eigenfunction and mode shapes. Here, the graphical behavior of the first four mode shapes of the torsional bar subject to different ends is given in Figure 2. The angular frequency is γ_m and amplitude becomes symmetric for odd modes $(m = 1, 3, 5, ...)$ and anti-symmetric for even modes $(m = 2, 4, 6, ...)$. Also, the free-free torsional bar represents vertical shifting in the plot. The distance between two successive crests of a wave is known as the wavelength. By increasing the number of modes, the wavelength of the wave decreases, and by relation $f \propto \frac{1}{\lambda}$, the frequency increases. The amplitude of the wave is defined as the corresponding distance from crest to crest or trough, and from these mode shapes, it is clear that amplitude and frequency are directly related to each other. Thus, in these graphs, the frequency is increasing. Consequently, the amplitude of a wave is also increasing.

Now, we will apply the root-finding technique to determine the dimensionless eigenvalue α for boundary conditions given in Eqs. (5)-(11).

Table 3. Eigenvalues and natural frequencies of free bar

m	$\beta_m = \frac{m\pi}{L}$	γ_m
1	π	0.46808
2	2π	0.936
3	3π	1.4043
4	4π	1.87239
5	5π	2.3404
6	6π	2.808
7	7π	3.2766
8	8π	3.7447
9	9π	4.2128
10	10π	4.6809

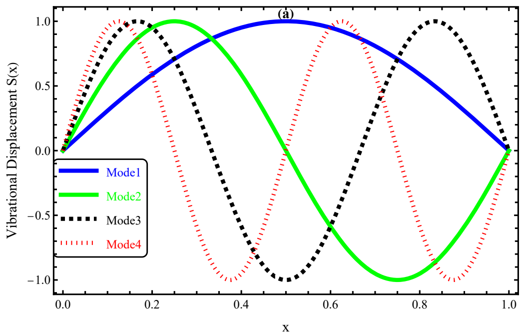

(a) Fixed ends

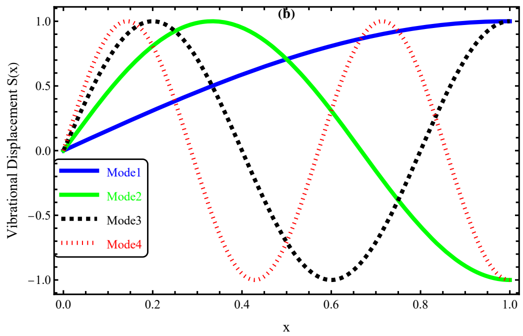

(b) Fixed-free ends

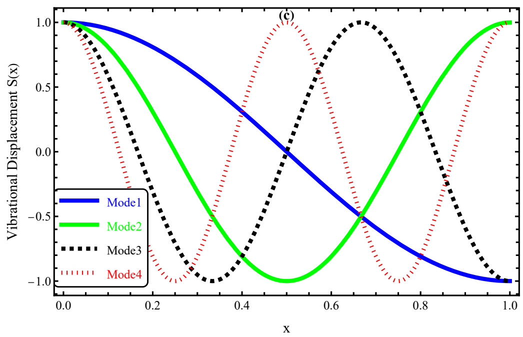

(c) Free ends

Figure 2. First four mode shapes of a bar

Here in Figure 3, red dots represent the zeros of the frequency equation, which are the desired eigenvalues. Due to the development of the dispersive relation, we are unable to determine eigenvalues explicitly. For this purpose, we will find these eigenvalues numerically. Now, eigenvalues and natural frequencies of the bar with $k_\phi = 0.1$, $G_x = 0.2$, $r = 1$, $P_I = 0.9$, and $L = 1$ are presented here in the form of figures of dispersive relations. Whereas, eigenvalues, eigenfrequencies, and characteristic parameters are computed in Tables 4–6.

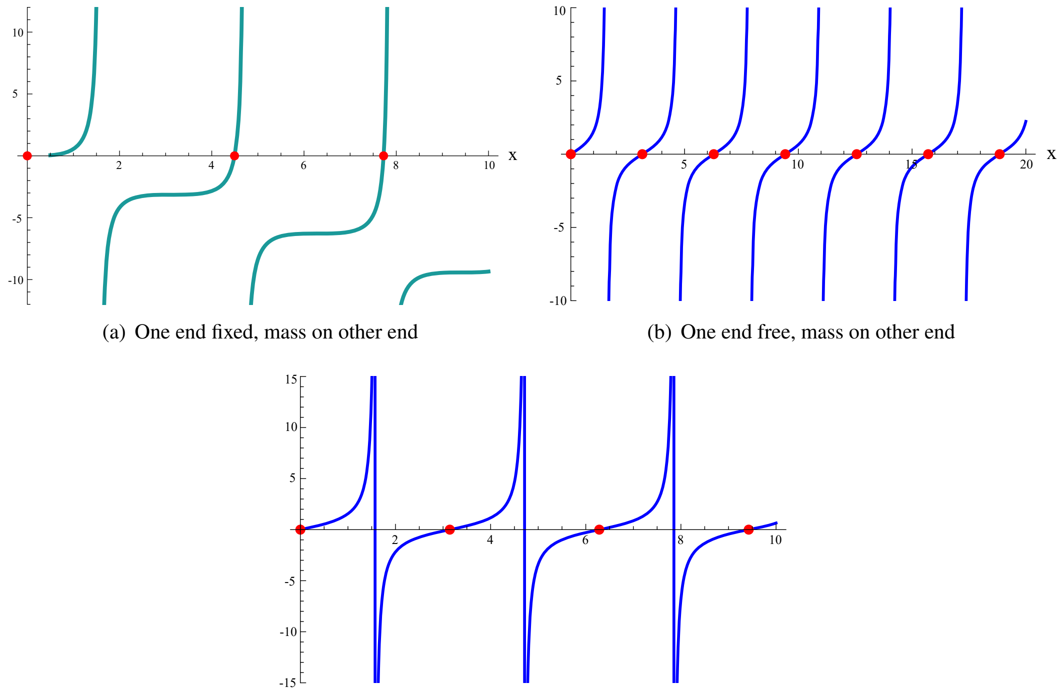

(a) One end fixed, mass on other end

(b) One end free, mass on other end

(c) Attached mass on both ends

Figure 3. Dispersive relation of a bar

Table 4. Eigenvalues and natural frequencies of fixed bar with mass attached at either end

m	α_m	γ_m
1	1.35	0.20
2	4.11	0.6126
3	6.99	1.04186
4	9.97	1.4850
5	12.998	1.9368
6	16.0654	2.3937
7	19.1531	2.8538
8	22.2545	3.3159
9	25.365	3.779
10	28.482	4.2438

Table 5. Eigenvalues and natural frequencies of free torsional bar having attached mass at either end

m	α_m	γ_m
1	0	0
2	2.88509	0.43008
3	5.79809	0.8643
4	8.75267	1.3047
5	11.74281	21.751
6	14.7771	2.2028
7	17.8315	2.658
8	20.9047	3.116
9	23.9918	3.576
10	27.0893	4.0328

Table 6. Eigenvalues and natural frequencies of free torsional bar having attached mass at both ends

m	α_m	γ_m	τ_m
1	0	0	0
2	2.16879	0.3233	0.361465
3	4.63008	0.69021	0.77168
4	7.354	1.09638	1.2258
5	10.2398	1.5265	1.77063

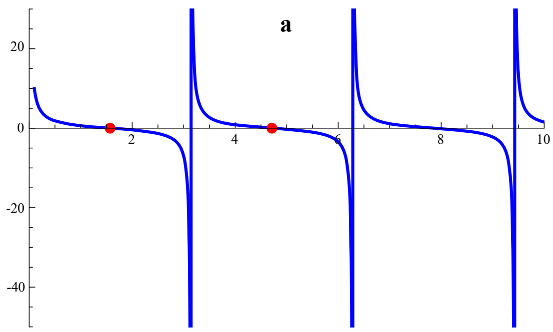

(a) One end fixed, and attached mass and spring on the other

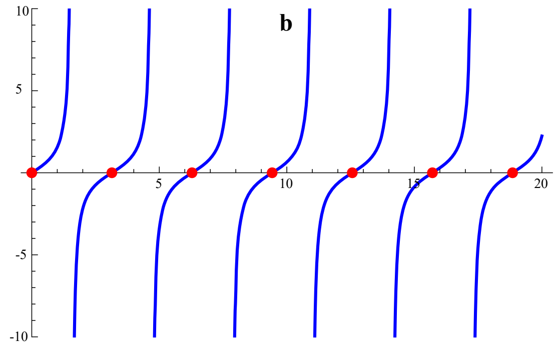

(b) One end free, attached mass and spring on other end

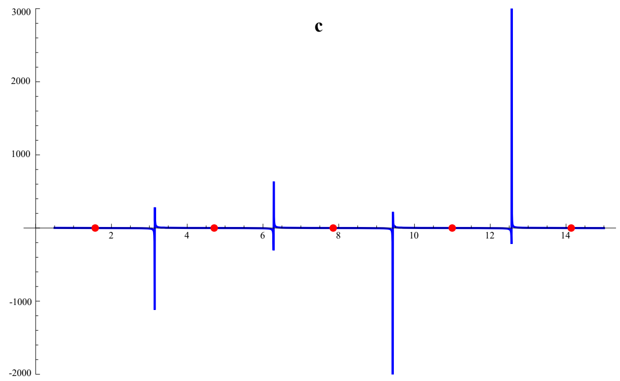

(c) Attached mass and spring on both ends

Figure 4. Dispersive relation of a bar

Table 7. Eigenvalues and natural frequencies of fixed torsional bar having attached mass and spring

m	α_m	γ_m
1	1.9112	0.2849
2	4.31395	0.643080
3	7.07032	1.0539
4	10.0012	1.4908
5	13.0163	1.9403

Table 8. Eigenvalues and natural frequencies of free torsional bar having attached mass and spring

m	α_m	γ_m
1	0.904234	0.134795
2	3.05386	0.45524
3	5.66148	0.84396
4	8.52125	1.27027
5	11.5015	1.71454

Table 9. Eigenvalues, natural frequencies and characteristics parameter of torsional bar having attached rigid masses and springs at both ends

m	α_m	γ_m
1	0	0
2	0.968	0.14431
3	1.5708	0.2342
4	2.46569	0.36756
5	4.67063	0.69625

Here, Tables 4–6 represent eigenvalues and natural frequencies of a bar at different ends that were calculated on the first five modes. If we compare all these values at different ends, all these values are almost equal. Also, in case one end of the bar is fixed or free, and the other end is attached with mass and springs, dispersive relations are generated and already presented in tables. In Figure 4, red dots represent roots of the frequency equation by considering parametric values $k_t = 9$, $k_\phi = 7$, $\lambda = 6$, and $L = 5$, respectively. Also, the corresponding eigenvalues and natural frequencies for these figures are presented here in Tables 7–9, respectively.

As we already discussed, for the linear algebraic system of equations obtained due to attached masses and springs, we obtained a highly transcendental frequency equation. We will apply numerical techniques to obtain non-dimensionalized eigenvalues by using the well-known software Mathematica, and corresponding to each eigenvalue, we have a mode shape. A few of these mode shapes are plotted against different parameters. Tables 7–9 represent values of different parameters, by carefully considering eigenvalues and natural frequencies of a bar representing different values at different ends. Now, the upcoming figures represent the first four mode shapes of a torsional bar having certain attached masses and springs. Figures 5–7 represent the first four mode shapes of a bar at different ends. These graphs are plotted against displacement x and vibrational displacement $S(x)$. By closely observing these graphs, the first four mode shapes of a free bar with mass attached at the left end, and a rigid mass at both ends, show approximately the same behavior.

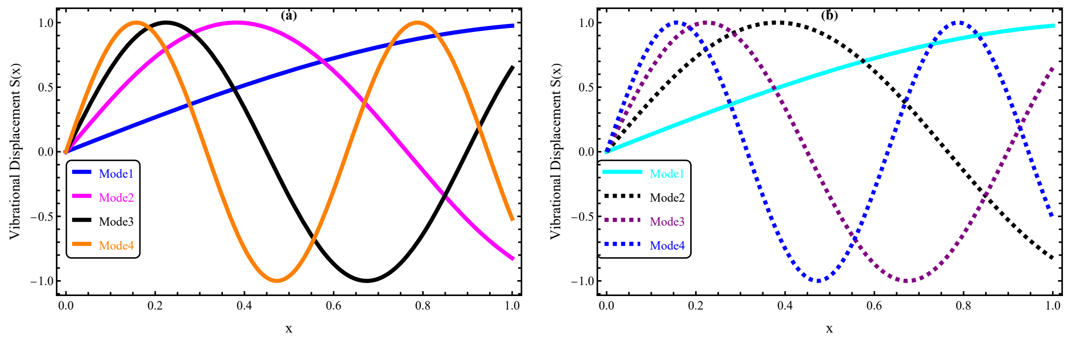

(a) Right end (b) Left end

Figure 5. First four mode shapes of a fixed torsional bar with rigid masses

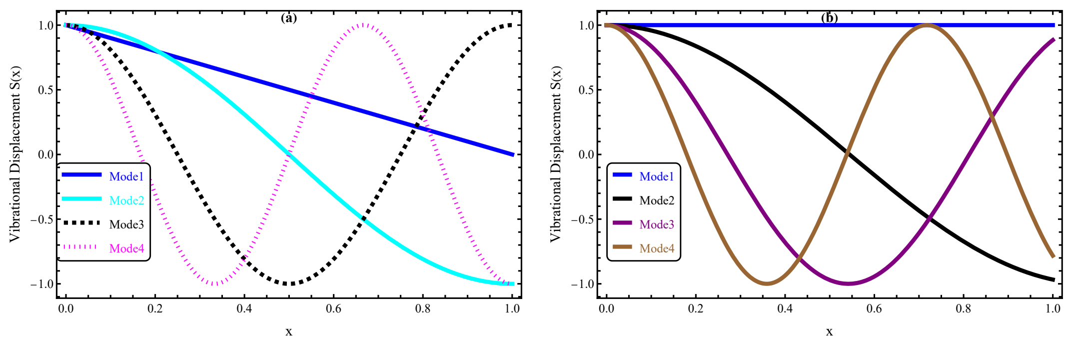

(a) Right end (b) Left end

Figure 6. First four mode shapes of a free torsional bar with rigid masses

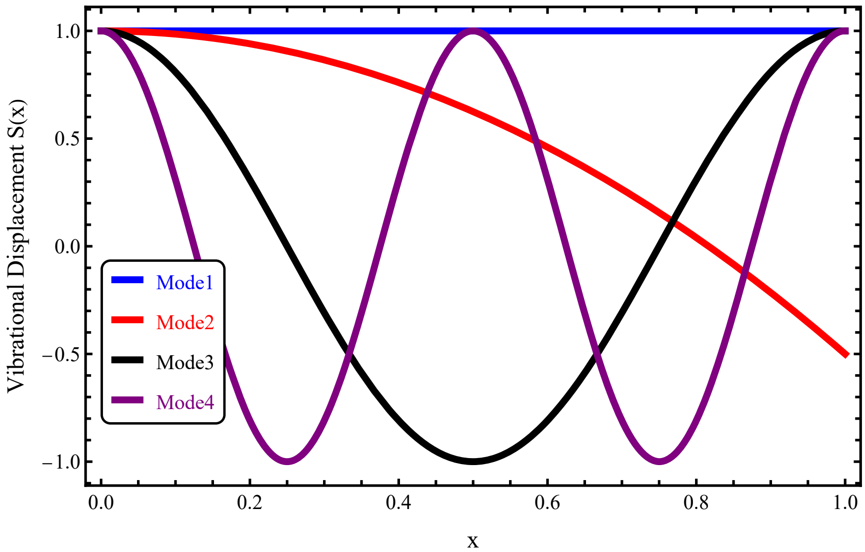

Figure 7. First four mode shapes of a torsional bar having rigid mass M at both ends

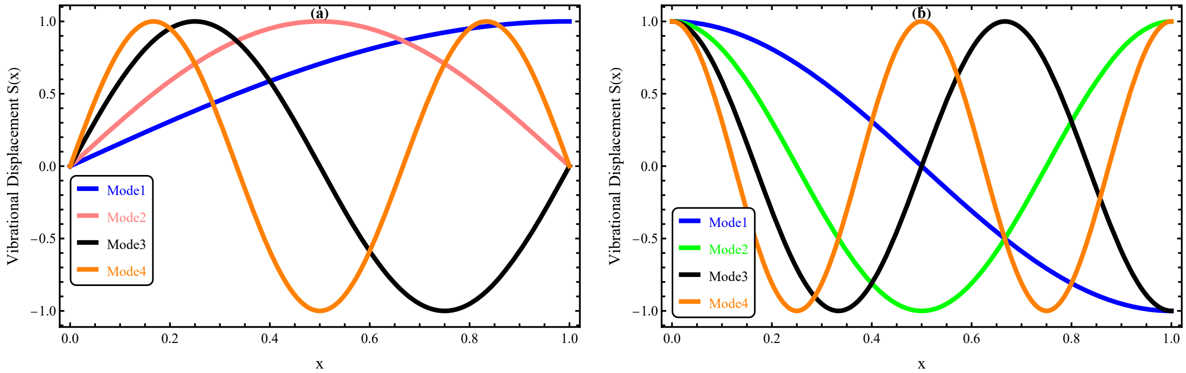

(a) Fixed end (b) free end

Figure 8. First four mode shapes of a torsional bar with rigid masses and springs

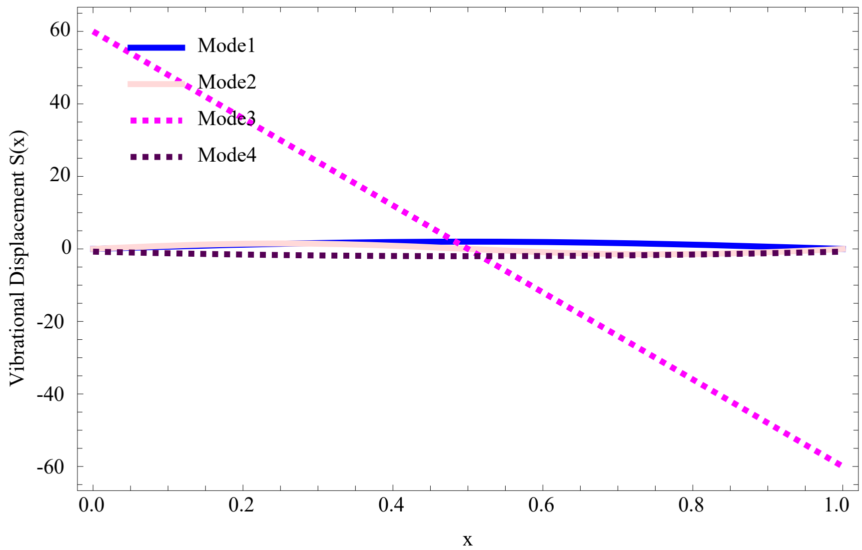

Figure 9. First four mode shapes of a torsional bar having attached mass M and spring

Figure 8 and Figure 9 represent symmetric and non-symmetric behaviour of mode shapes. Wavelength is the distance between two consecutive crests of a wave. So, from the above graphs, it is witnessed that by increasing the number of modes, the wavelength decreases, and by relation $f \propto \frac{1}{\lambda}$, corresponding frequencies increase. Also, the amplitude of the wave is defined as the distance from the rest position to the crest or trough, and the amplitude of the wave increases with an increase in frequency and vice versa.

From the boundary conditions given in Eq. (13), it is observed that when dampers are connected along with mass and spring, complexity occurs in the bar, which produces an infinite number of complex eigenvalues and eigenfunctions. Some of them are presented below in tabular form and also, the graphical behavior of the dispersive relation of bar and complex roots is presented below. These complex roots are basically our eigenvalues.

Figure 10 represents the dispersive relation of a bar with attached mass, springs, and dampers. Due to dampers, the complexity arises. and both complex and real roots get generated. Here, red dotted lines represent complex roots, and green dotted lines correspond to real roots. The eigenvalues and the characteristics parameter of the torsional bar having attached rigid masses, springs, and dampers at both ends are listed in Table 10.

Now, complex roots are generated due to viscous damping on the bar. Corresponding to these complex roots, which are our eigenvalues, complex eigenfunctions are also generated. The graphical behavior of the first four mode shapes of the torsional bar is presented here in the figures below, respectively. Here, every point on a real line represents a real number, similarly, every point on a complex plane represents a complex number. In Figure 11, graphs are plotted against displacement x and vibrational displacement ω(x). The blue line shows the real part and the yellow line represents the imaginary part of each mode shape. We observed that the complex root gets generated due to the attached viscous dampers at the end of the bar. Each real number can be represented by a point in the real line, and each point in the real line is a real number. Likewise, each complex number can be represented by a point in the complex plane, and each point in the complex plane is a complex number.

A complex plane has two perpendicular axes, the real and the imaginary one. Here, we observed that both real and imaginary parts represent symmetric and antisymmetric behavior. In the above Figure 11, the first and third modes are symmetric while the second and fourth modes are antisymmetric. We noticed that in the case of a real wave, there is a decrease in the wavelength, and inversely related frequency increases, and so does the amplitude. An opposing behavior occurred for the imaginary wave as we move with distance, the wavelength increases, such that frequency and amplitude get diminished.

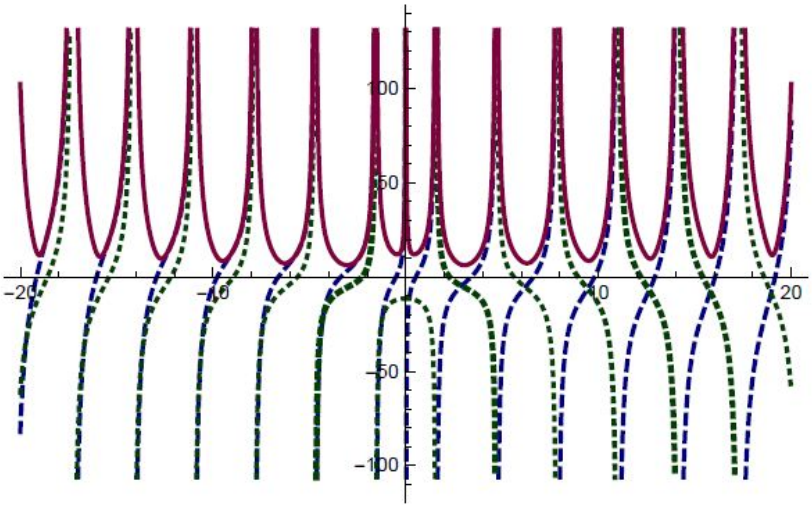

Figure 10. Dispersive relation of a torsional bar with mass, springs, and dampers on both ends

Table 10. Eigenvalues and characteristics parameter of torsional bar having attached rigid masses, springs, and dampers at both ends

m	ψ	η
1	$2.3 \times 10^{-17} + 1.21\iota$	4.55×10^{-15}
2	$3 + 0.7\iota$	$0.68 + 0.07\iota$
3	$6.3 + 0.5\iota$	$0.42 - 0.22\iota$
4	$9.5 + 0.4\iota$	$0.255 - 0.23788\iota$
5	$12.7 + 0.36\iota$	$0.16 - 0.22\iota$
6	$15.9 + 0.30\iota$	$0.09 - 0.19\iota$

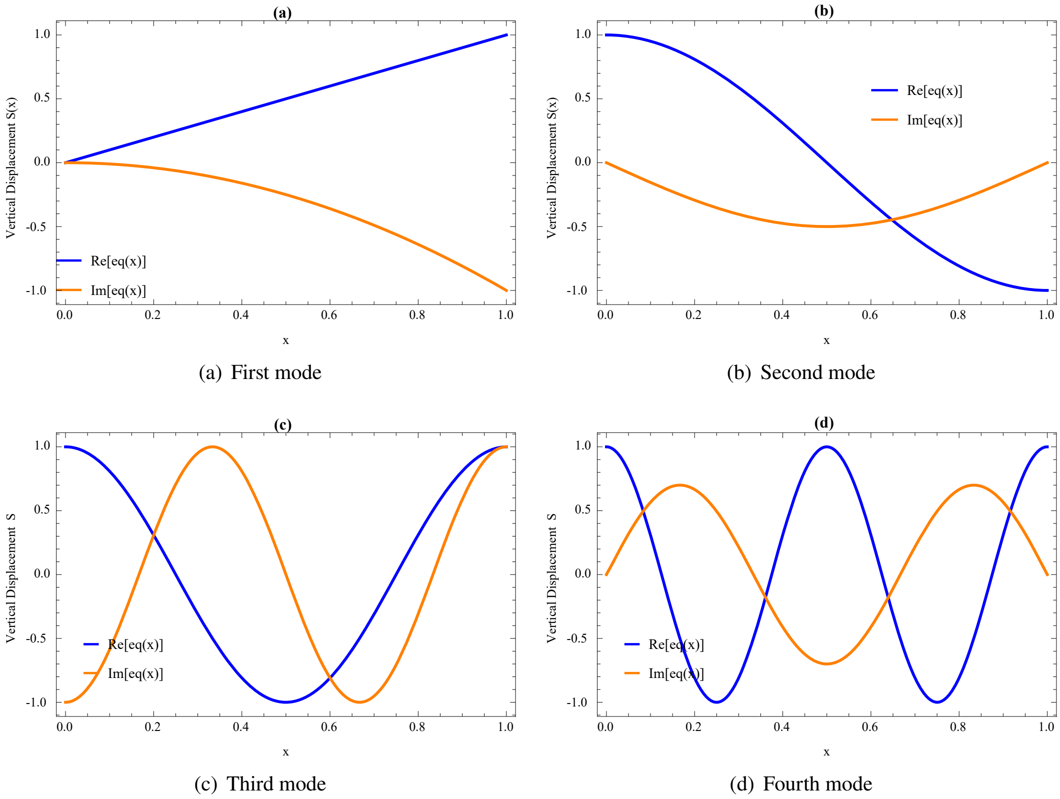

(a) First mode

(b) Second mode

(c) Third mode

(d) Fourth mode

Figure 11. First four mode shapes of a free torsional bar with rigid masses, springs, and dampers

5 Conclusion

We examined how the various models' eigenfrequencies and characteristic equations were affected by their geometrical and physical characteristics. Because it is impossible to find explicitly generated eigenvalues, the FEM method was used to calculate the fixed and free ends' eigenfrequencies, which were found to be similar. Dispersive relations are also generated when masses and springs are attached to either or both ends of the bar.

An exact and direct modeling method is suggested in this article. For an elastic torsional bar with varying foundations, including masses, linear springs, and viscous dampers, one can easily determine its natural frequencies and mode shapes by using the FEM as presented in this paper.

It was discovered that, for the first four eigenmodes and eigenfrequencies, the results demonstrated remarkable agreement with the finite element results. This implies that for similar issues, the finite element scheme is a great method for generating precise eigenmodes and mode shapes.

When dampers are attached along with mass and springs at both ends of the elastic bar, complexity arises due to viscous damping that produces both real and complex roots, resulting in complex eigenvalues that were impossible to determine numerically. For this reason, Mathematica was used to analyze the graphical behavior of mode shapes subject to various considerations. Nevertheless, viscous damping had a greater influence on the eigenfrequencies than attached masses and springs.

Future Direction: A possible direction for future work is to consider the aerodynamic damping, which basically involves the non-linearity in governing equations that can be handled through numerical techniques like FEM.

Data Availability

The data used to support the research findings are available from the corresponding author upon request.

Conflicts of Interest

The authors declare no conflict of interest.

References

[1] W. Thomson, *Theory of Vibration with Applications*, 1st ed. London: CRC Press, 1993.

[2] W. Wang, T. Yang, X. Chen, and X. Yao, "Vibration energy harvesting using a piezoelectric circular diaphragm array," *IEEE Trans. Ultrason. Ferroelectr. Freq. Control*, vol. 59, no. 9, pp. 2022–2026, 2012. https://doi.org/10.1109/TUFFC.2012.2422

[3] H. Bachmann, *Vibration Problems in Structures: Practical Guidelines*. Springer Science & Business Media, 1995.

[4] A. Muszynska, "Vibrational diagnostics of rotating machinery malfunctions," *Int. J. Rotating Mach.*, vol. 1, no. 3-4, pp. 237–266, 1995.

[5] A. Shabana, *Vibration of Discrete and Continuous Systems*. New York: Springer, 1997.

[6] J. Angeles, *Dynamic Response of Linear Mechanical Systems: Modeling, Analysis and Simulation*. Springer Science & Business Media, 2011.

[7] J. Yang, J. C. Leng, J. T. Zhou, R. Chen, K. Yu, Z. M. Jiang, Y. Zou, Z. Y. Zhang, and J. Du, "Study on the impact of vehicle-induced vibration on the flexural behavior of UHPC joints in widened bridges," *Urban Lifeline*, vol. 2, no. 1, p. 20, 2024. https://doi.org/10.1007/s44285-024-00028-x

[8] X. X. Cheng, J. Dong, S. S. Cao, X. L. Han, and C. Q. Miao, "Static and dynamic structural performances of a special-shaped concrete-filled steel tubular arch bridge in extreme events using a validated computational model," *Arab. J. Sci. Eng.*, vol. 43, no. 4, pp. 1839–1863, 2018. https://doi.org/10.1007/s13369-017-2771-0

[9] T. A. Grøv, "Fatigue of flexible risers considering alternative constitutive models," Master's thesis, Institutt for Marin Teknikk (IMT), Norway, 2014.

[10] H. Wu and G. Wu, "Driveline torsional analysis and clutch damper optimization for reducing gear rattle," *Shock Vib.*, vol. 2016, no. 1, p. 8434625, 2016. https://doi.org/10.1155/2016/8434625

[11] J. Qu, W. Shi, Z. Chen, R. Yuan, J. Liu, Y. Zhao, and N. Guo, "Nonlinear modeling and torsional vibration analysis of heavy-duty vehicle powertrain system during acceleration," *Adv. Mech. Eng.*, vol. 16, no. 7, p. 16878132241263936, 2024. https://doi.org/10.1177/16878132241263936

[12] L. Murawski and M. Dereszewski, "Theoretical and practical backgrounds of monitoring system of ship power transmission systems' torsional vibration," *J. Mar. Sci. Technol.*, vol. 25, no. 1, pp. 272–284, 2020. https://doi.org/10.1007/s00773-019-00646-z

[13] X. Chen, D. Peng, J. Hu, C. Li, S. Zheng, and W. Zhang, "Adaptive torsional vibration active control for hybrid electric powertrains during start-up based on model prediction," *Proc. Inst. Mech. Eng. Part D*, vol. 236, no. 10-11, pp. 2219–2229, 2022. https://doi.org/10.1177/0954407021105617

[14] S. Chen and M. H. Hu, "Active torsional vibration suppression of integrated electric drive system based on optimal harmonic current instruction analytic calculation method," *Mech. Mach. Theory*, vol. 180, p. 105136, 2023. https://doi.org/10.1016/j.mechmachtheory.2022.105136

[15] A. Tariq, H. G. Kadıoğlu, B. Uzun, B. Deliktaş, and M. Ö. Yaylı, "Semi-analytical and machine learning approaches for investigating the torsional vibration behavior of nano-sized viscoelastic tubes," *Mech. Adv. Mater. Struc.*, pp. 1–21, 2025. https://doi.org/10.1080/15376494.2025.2471036

[16] A. Sharma, K. Abid, S. Srivastava, A. F. B. Velasquez, and C. Teodoriu, "A review of torsional vibration mitigation techniques using active control and machine learning strategies," *Petroleum*, vol. 10, no. 3, pp. 411–426, 2024. https://doi.org/10.1016/j.petlm.2023.09.007

[17] D. F. Ledezma-Ramírez, P. E. Tapia-González, N. Ferguson, M. Brennan, and B. Tang, "Recent advances in shock vibration isolation: An overview and future possibilities," *Appl. Mech. Rev.*, vol. 71, p. 060802, 2019. https://doi.org/10.1115/1.4044190

[18] H. Ç. Sezgen and M. Tinkir, "Optimization of torsional vibration damper of cranktrain system using a hybrid damping approach," *Eng. Sci. Techn., Int. J.*, vol. 24, no. 4, pp. 959–973, 2021. https://doi.org/10.1016/j.jestch.2021.02.008

[19] Y. Cao, H. Yao, H. Li, and J. Dou, "Torsional vibration dynamics of a gear-shafting system attaching a nonlinear energy sink," *Mech. Syst. Signal Process.*, vol. 176, p. 109172, 2022. https://doi.org/10.1016/j.ymssp.2022.109172

[20] F. Liang, W. H. Xu, and Z. Q. Chen, "Flexural–torsional vibration reduction of an eccentric phononic crystal pipe conveying fluid," *J. Fluids Struc.*, vol. 120, p. 103904, 2023. https://doi.org/10.1016/j.jfluidstructs.2023.103904

[21] Y. Cao, G. Yan, J. Lu, and W. Zhang, "Suppression of multi-modal torsional vibration of the long-shafting rotor system with nonlinear piecewise NES," *Int. J. Non Linear Mech.*, vol. 159, p. 104617, 2024. https://doi.org/10.1016/j.ijnonlinmec.2023.104617

[22] J. Dou, H. Yao, H. Li, D. Gao, and S. Han, "Torsional vibration suppression of a spline-rotor system using a multi-stable nonlinear energy sink," *Mech. Syst. Signal Process.*, vol. 211, p. 111240, 2024. https://doi.org/10.1016/j.ymssp.2024.111240

[23] K. Ma, J. Du, H. Zhang, Y. Liu, and X. Chen, "A comparative study on the torsional vibration suppression of

rotor system using variable steady state nonlinear energy sink," *Chaos, Solitons Fract.*, vol. 185, p. 115144, 2024. https://doi.org/10.1016/j.chaos.2024.115144

[24] K. Radhakrishnan, A. G. Antony, K. Rajaguru, and B. Sureshkumar, "Torsional vibration analysis of torsion bar spring for off road vehicle driver seat," *Mater. Today Proc.*, vol. 21, pp. 669–672, 2020. https://doi.org/10.1016/j.matpr.2019.06.736

[25] S. Laine, U. Hakonen, H. Hartikainen, and R. Viitala, "Frequency domain solution method for electromagnetic influence analysis on torsional vibrations," *J. Sound Vib.*, vol. 596, p. 118780, 2025. https://doi.org/10.1016/j.jsv.2024.118780

[26] A. E. H. Love, *A Treatise on the Mathematical Theory of Elasticity*. Courier Corporation, 1994.

[27] A. W. Leissa and M. S. Qatu, *Vibrations of Continuous Systems*. New York, NY, USA: McGraw-Hill, 2011.

[28] S. S. Rao, *Vibration of Continuous Systems*. John Wiley & Sons, 2019.

[29] L. L. Ke, Y. S. Wang, J. Yang, and S. Kitipornchai, "Free vibration of size-dependent mindlin microplates based on the modified couple stress theory," *J. Sound Vib.*, vol. 331, no. 1, pp. 94–106, 2012. https://doi.org/10.1016/j.jsv.2011.08.020

[30] B. Akgöz and Ö. Civalek, "Longitudinal vibration analysis for microbars based on strain gradient elasticity theory," *J. Vibration Control*, vol. 20, no. 4, pp. 606–616, 2014. https://doi.org/10.1177/1077546312463752

[31] V. Dimosthenis, "Longitudinal vibration analysis of strain gradient elastic bar with various boundary conditions," *J. Appl. Eng. Sci.*, vol. 22, no. 3, pp. 665–680, 2024. https://doi.org/10.5937/jaes0-51432

[32] W. Xu, W. D. Zhu, S. A. Smith, and M. S. Cao, "Structural damage detection using slopes of longitudinal vibration shapes," *J. Vib. Acoust.*, vol. 138, no. 3, p. 034501, 2016. https://doi.org/10.1115/1.4031996

[33] R. Barretta, S. A. Faghidian, and R. Luciano, "Longitudinal vibrations of nano-rods by stress-driven integral elasticity," *Mech. Adv. Mater. Struct.*, vol. 26, no. 15, pp. 1307–1315, 2019. https://doi.org/10.1080/15376494.2018.1432806

[34] W. Xu, W. Zhu, Z. Su, M. Cao, and H. Xu, "A novel structural damage identification approach using damage-induced perturbation in longitudinal vibration," *J. Sound Vib.*, vol. 496, p. 115932, 2021. https://doi.org/10.1016/j.jsv.2021.115932

[35] E. Demir, M. Sayer, and H. Callioglu, "An approach for predicting longitudinal free vibration of axially functionally graded bar by artificial neural network," *Proc. Inst. Mech. Eng., Part C*, vol. 237, no. 10, pp. 2245–2255, 2023. https://doi.org/10.1177/09544062221141246

[36] Y. Zhao, F. Guo, and D. Xu, "Longitudinal vibration responses of a double-rod system coupled through a nonlinear element," *Nonlinear Dyn.*, vol. 112, no. 3, pp. 1759–1778, 2024. https://doi.org/10.1007/s11071-023-09138-7

[37] T. Shang, Q. Huang, and Y. Wang, "Vibration reduction and energy harvesting on the ship thrust bearing unit excited by a measured shaft longitudinal vibration using NES-GMM," *Ocean Eng.*, vol. 294, p. 116914, 2024. https://doi.org/10.1016/j.oceaneng.2024.116914

[38] S. Rosenberg and O. Shoshani, "Shape optimization of a curved mechanical beam for transverse vibrations amplification via nonlinear interaction with longitudinal vibrations," *J. Sound Vib.*, vol. 599, p. 118908, 2025. https://doi.org/10.1016/j.jsv.2024.118908

[39] S. Shamsi and L. Prikazchikova, "Low-frequency longitudinal vibrations of a fluid-loaded elastic layer," *Symmetry*, vol. 17, no. 1, p. 119, 2025. https://doi.org/10.3390/sym17010119

[40] H. Ma, "Exact solutions of axial vibration problems of elastic bars," *Int. J. Numer. Methods Eng.*, vol. 75, no. 2, pp. 241–252, 2008. https://doi.org/10.1002/nme.2254

[41] H. R. H. Kabir, "On free vibration response and mode shapes of arbitrarily laminated rectangular plates," *Compos. Struct.*, vol. 65, no. 1, pp. 13–27, 2004. https://doi.org/10.1016/j.compstruct.2003.10.001